MATEC Web of Conferences **145**, 03004 (2018) https://doi.org/10.1051/matecconf/201814503004
*NCTAM 2017*

# A case study of the plasma in the magneto-sheath using the numerical magnetosheath-magnetosphere model and THEMIS measure-ments

*Polya* Dobreva[1,*], *Olga* Nitcheva[1], *Monio* Kartalev[1]

[1] Institute of Mechanics, Bulgarian Academy of Sciences, Acad. G. Bonchev Str., block 4, Sofia, Bulgaria

**Abstract.** This paper presents a case study of the plasma parameters in the magnetosheath, based on THEMIS measurements. As a theoretical tool we apply the self-consistent magnetosheath-magnetosphere model. A specific aspect of the model is that the positions of the bow shock and the magnetopause are self-consistently determined. In the magnetosheath the distribution of the velocity, density and temperature is calculated, based on the gas-dynamic theory. The magnetosphere module allows for the calculation of the magnetopause currents, confining the magnetic field into an arbitrary non-axisymmetric magnetopause. The variant of the Tsyganenko magnetic field model is applied as an internal magnetic field model. As solar wind monitor we use measurements from the WIND spacecraft. The results show that the model quite well reproduces the values of the ion density and velocity in the magnetosheath. The simlicity of the model allows calulations to be perforemed on a personal computer, which is one of the mean advantages of our model.

## 1 Introduction

The magnetosheath plays very important role in the solar wind–magnetosphere-ionosphere interaction. In the magnetosheath the solar wind slows down, as its density and temperature increase. The Earth's magnetosheath is a transitional region, through which energy is transferred from the Sun to the Earth's atmosphere. Therefore, understanding the mechanism of energy transfer requires the creation of adequate magnetosheath models.

The pioneering work in description the magnetosheath dynamics was the model of Spreiter [1]. For given input parameters – the Mach number and polytropic index, and a given magnetopause shape, the model calculates the plasma parameters in the magnetosheath - density, velocity and temperature. The bow shock position is also calculated as a part of the solution. Later, the model was further developed including the distribution of the magnetic field in the magnetosheath [2]. As the solution (and in particular the velocity distribution) is known, the magnetic field in the magnetosheath can

* Corresponding author: polya2006@yahoo.com

easily be calculated from the magnetic induction equation. However, the model has some limitations, such as the assumption of axisymmetric bow shock shape and a given prescribed shape of the magnetopause [3].

Execution of large global MHD simulations in the domains of the solar wind to the atmosphere requires significant computing resources. In recent decades, the advances of computer technology made possible the creation of codes, that solve the magnetohydrodynamics equations. Examples of these simulations are the Ogino model [4], GUMICS model (Grand Unified Magnetosphere–Ionosphere Coupling Simulation) [5]. Other well known codes include OpenGGCM ( Open General Geospace Circulation Model) [6], LFM model (Lyon–Fedder–Mobarry) [7], SWMF (Space Weather Modelling Framework) [8] which is based on BATS-R-US MHD code [9].

The numerical magnetosheath-magnetosphere model was developed based on a simpler gas-dynamic approach, that is capable of describing the main characteristics of the megnetosheath without the need for extreme computational resources. The model is able to reproduce the real 3D geometry of the magnetosheath boundaries - bow shock (BS) and magnetopause (MP), including indentations around the cusp at the magnetopause. The model also accounts for the down-dusk asymmetries in the tail magnetopause and north-south displacement, induced by the dipole tilt variations. The accuracy and relative simplicity of our model make it an accessible instrument to describe the large-scale magnetosheath properties.

The model was previously applied to study the ion flux distribution in the magnetosheath, using the Interball-1 measurements mainly – [10, 11].

The aim of this paper is to test the model capabilities on recent data from the THEMIS mission. Parameters to be interpreted are the ion velocity and ion density in a case of THEMIS passage through the magnetosheath. On 10-11 June 2009 the satellite crosses the equatorial magnetosheath close to the terminator (x=0) plane.

A brief description of the model will be given in Section 2. In Section 3 we will present the solar wind data, the magnetosheath data and a comparison between the model calculations and the experiment.

## 2 Short description of the model

Here, we will present only in general outline the numerical scheme that has been applied. The interaction of the solar wind with the Earth's magnetosphere is described by the self-consistent magnetosheath-magnetosphere model. A single-fluid model is implemented in the magnetosheath, while in the magnetosphere we employ a magnetic field model. The flow in the magnetosheath is described by the compressible 3D Euler equations of a perfect gas. The system of equations is solved by a variant of the grid-characteristic methods [12], which are often used in gas-dynamics. The magnetic field is represented as a variant of the magnetosphere model of Tsyganenko -T96 or T01 [13, 14]. The Tsyganenko model is modified to allow for a particular, non-axisymmetric shape of the boundary. The magnetopause is approximated as a surface of a tangential discontinuity.

The imposed boundary conditions are the Rankine-Hugoniot relations. They are reduced to the pressure balance equation at the magnetopause. The equation allows us to obtain specific magnetopause geometry, including indentations at the cusp, north-south and dawn-dusk asymmetries. Thus, there is no need of rescaling the satellite trajectories or the magnetosheath thickness in order to achieve a coincidence with the boundary positions.

Input data are plasma and magnetic field properties of the incoming flow, including the dynamic pressure $P_d$, sonic Mach number M, $B_y$ and $B_z$ components of the Interplanetary Magnetic Field (IMF), polytropic coefficient $\gamma$.

The Dst index, based on the Kyoto Web page, and the dipole tilt are also set at the beginning of a simulation. A more detailed description of the numerical algorithm, used in the calculations, can be found in previous papers [10, 11, 15, 16].

## 3 Numerical results

### 3.1 Input data

On 10-11 June 2009 the ACE spacecraft [17] is in orbit around Lagrange L1 point. Since during this interval the ACE density measurements are not available, we will use measurements from the WIND spacecraft [18] as input data. The WIND spacecraft is also

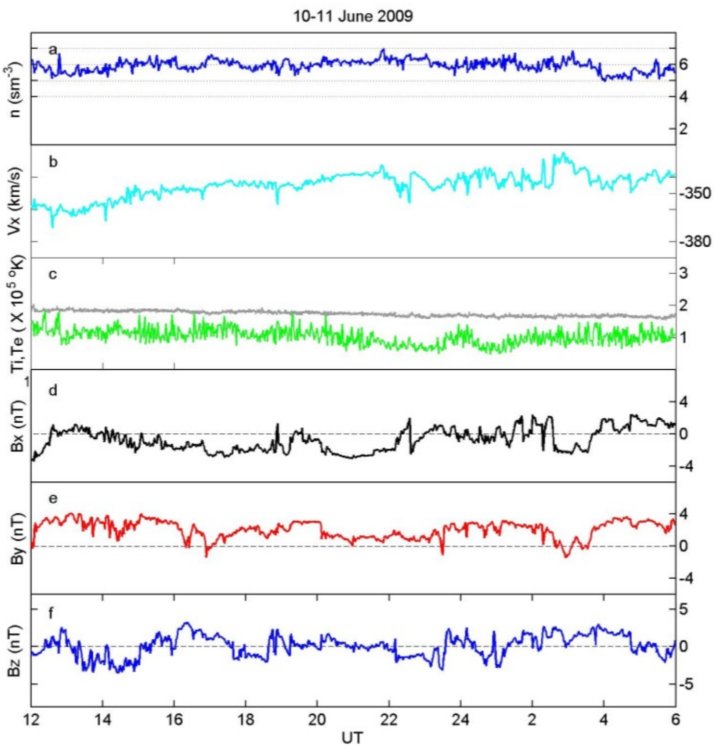


**Fig. 1.** Input solar wind data on 10-11 June 2009 : a) ion number density; b) $V_x$ component of the ion velocity; c) ion temperature $T_i$ (green) and electron temperature $T_e$ (gray); d) $B_x$, e) $B_y$ and f) $B_z$ GSM (Geocentric Solar Magnetospheric) components of the interplanetary magnetic field. The data are not shifted in time.

in the pristine solar wind, located at about 261 $R_E$ (Earth radii) from the Earth. The propagation time from WIND to the Earth varies between 79 min (at 17:00 UT) and 82 min (at 2:30 UT on 11 June). The plasma and magnetic field measurements, conducted by the WIND satellite on 10-11 June 2009 are presented in Fig.1. During this interval the solar wind conditions are quiet as the plasma parameters vary in a narrow range. The ion density is almost constant – about 6 $sm^{-3}$, similarly to the electron temperature, that is about 1.9-1.8 x $10^5$ ºK. The velocity varies in the range -330~ -350 km/s, the ion temperature is 1.3 x $10^5$ ºK at the beginning of the interval, drops to about 0.8 x $10^5$ ºK at the interval [22:00-02:00 UT] on 10-11 June, and rises to 1.0 x $10^5$ ºK after 2:00 UT on 11 June.

The input density, velocity and electron temperature are based on WIND/SWE (Solar Wind Experiment) device [19], the ion temperature – on WIND 3DP (3D Plasma analyzer) [20]. The Interplanetary magnetic field is determined by WIND/MFI (Magnetic Field Investigation) [21]. The time resolution is 1.5 min for the density, the velocity and the ion temperature, 1 min for the magnetic field and 12s for the electron temperature.

### 3.2 Magnetosheath measurements

THEMIS (Time History of events and Macroscale Interaction during Substorms) is a constellation of five probes, which primary objective is to study the energy release during the substorms in the magnetosphere [22, 23]. Launched on February 2007, they carried identical instrumentation aboard. For the first months of the mission, they operated in so called coast phase, moving as a tight cluster in elliptical orbit with an apogee of 15.4 $R_E$. After the preliminary phase, that continued until September 2007, they were separated from each other and their baseline mission of scientific observations began.

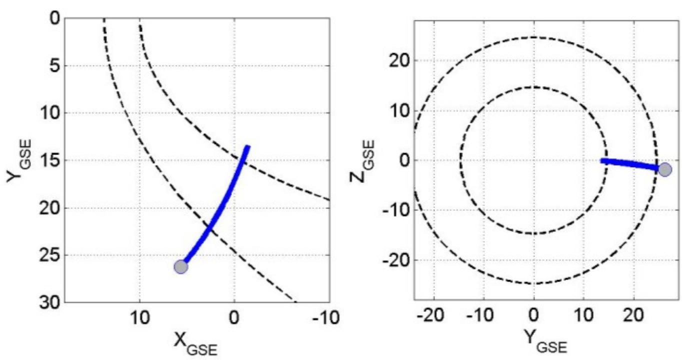


**Fig. 2.** Projection of the TH B orbit on the (X,Y) and (Y,Z) GSE (Geocentric Solar Ecliptic) coordinate planes, during the interval [12:00-06:00] UT on 10-11 June 2009. The point denotes the beginning of the interval. The inner curve represents the magnetopause from the Shue 97 model [24], calculated with average solar wind parameters of $P_d$=2 nPa, and $B_Z$=0 nT, while the outer curve is the bow shock, calculated by our model for the above mentioned magnetopause boundary.

From 15 April to 15 June 2009 they were on radiation belt mission and moved in strictly elliptic orbits with apogees on the dusk side. The outer probes P1(TH B) and P2 (TH C) have an apogee of 30 $R_E$ and 20 $R_E$ respectively. The inner three probes P3 (TH D), P4 (TH E) and P5 (TH A) moved close to each other with an apogee of 12 $R_E$.

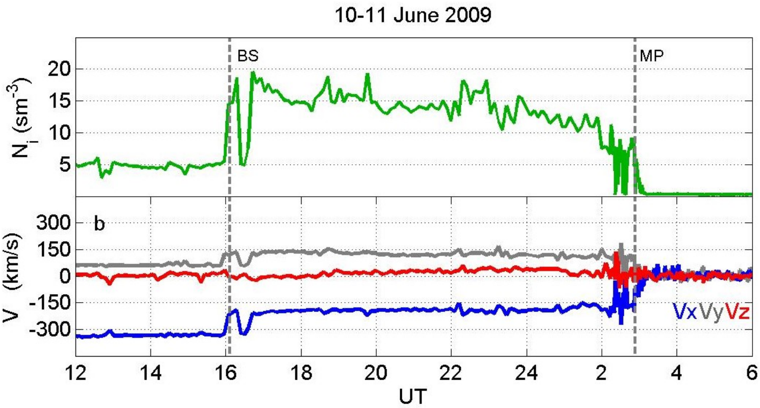


**Fig. 3.** Plasma measurements, conducted onboard THEMIS B satellite on 10-11 June 2009: a) ion number density; b) $V_x$ (blue) ,$V_y$ (gray) and $V_z$ (red) GSM component of the measured ion velocity. The vertical dashed lines denote the moments of the BS and MP crossings.

On 10-11 June 2009 all five satellites moved on the dusk side, as the inner three probes P3, P4 and P5 stayed in the magnetosphere. The outer P2 probe only partially crossed the magnetosheath. We will use data from the outermost P1 probe, which on 10-11 June crossed the magnetosheath entirely. In this paper we use TH B notation to refer to THEMIS P1 probe, which is most commonly used in the literature.

Fig. 2. shows the orbit of TH B on two perpendicular GSE planes, corresponding to the interval [12:00 – 06:00 UT] on 10-11 June 2009. For clarity, exemplary shapes of the bow shock and magnetopause are also shown. The magnetopause shape is the form of Shue 1997 [24], corresponding to mean values of dynamic pressure $P_d$=2. nPa and IMF $B_z$ = 0.nT. The bow shock is that calculated by out model for the given magnetopause shape and given input parameters of Mach=8 and polytropic index $\gamma$ =2. Most of the time TH B stayed close to equatorial GSE plane, meanwhile moving earthward and slowly northward.

The ion density and velocity, based on TH B on 10-11 June 2009 are visualized in Fig. 3. The jump of the density and velocity shows, that the satellite crosses the BS at 16:03 UT and after 2:50 UT (11 June) it stayed entirely in the magnetosphere. The density drop at the short interval [16:20-16:40 UT] is associated with the satellite's re-entering in the solar wind. After 16:40UT the spacecraft remained entirely in the magnetosheath. Since our purpose is not the investigation of multiple crossings we will consider the magnetosheath passage from the moment of the first BS crossing at 16:03 UT. During the interval [2:20-2:50 UT] on 11 June the satellite encountered both magnetosheath and magnetospheric plasma, as after 2:50UT TH B remained in the magnetosphere. The data, shown on the plot are based on TH B/ESA (Electrostatic Analyzer) instrument [25] and have a time resolution of 6.5 min.

### 3.3 Model results

Our purpose is to calculate the values of the plasma parameters along the satellite trajectory in the magnetosheath and to compare them with the measurements. Here we apply the algorithm, that was already used in our previous papers, considering satellite data interpretation [10, 11, 16].

We divide the whole interval into three subintervals [16:03-18:30 UT], [18:30-22:30 UT], [22:30-2:50 UT] and make the calculations with sets of input parameters, corresponding to the time moments 16:45UT, 22:00UT (on 10 June) and 2:30 UT (on 11

June). Then values in each individual interval are concatenated to give the solution in the entire interval. Parameters, applied in the simulations are given in Table 1, the ratio of specific heats is γ=2.

**Table 1.** Solar wind data used as an input to the model: dynamic pressure $P_d$ (in nPa), Mach number, $B_y$ and $B_z$ GSM components (in nT), Dst index and dipole tilt angle (in degrees).

| UT | $P_d$ | M | $B_y$ | $B_z$ | Dst | tilt |
|---|---|---|---|---|---|---|
| 16:45 | 1.26 | 4.96 | 3.0 | 1.0 | 4 | 32.6° |
| 22:00 | 1.21 | 4.99 | 1.2 | 0.4 | 1 | 24.7° |
| 02:30 | 1.1 | 5.13 | 2.5 | 0.1 | 4 | 14.8° |

Fig. 4 presents distributions of the density a) and velocity b) in the magnetosheath, calculated at the moment of MP crossing 2:30 UT. The plain, that passes through the satellite location at the moment of the MP crossing is shown. The satellite orbit is also added. The blue point denotes the satellite position when it finally enters into the magnetosphere at 2:50 UT. We see, that the observed moment of MP crossing is in good coincidence with the model-calculated boundary.

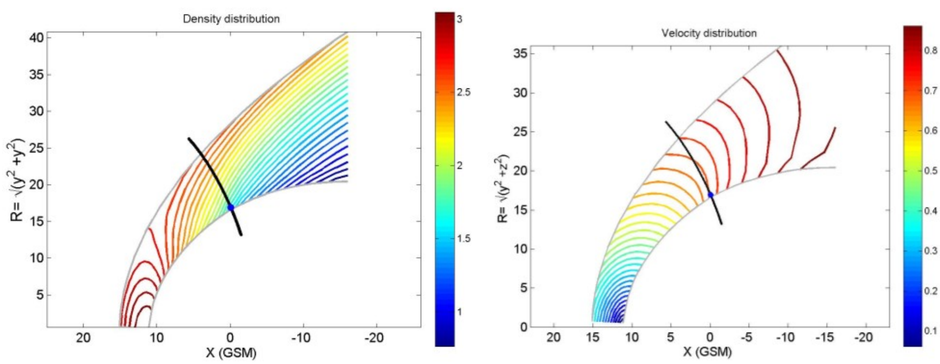


**Fig. 4.** Distribution of the ion density (left) and the velocity (right) in the magnetosheath. The parameters are presented in non dimensional units. The thick black line depicts the orbit projection of TH B from [12:00-06:00 UT] on 10-11 June 2009.

The comparison of the results of the calculation of the plasma velocities with the ones, measured onboard TH B is shown in Fig. 5. The directional components $V_x$, $V_y$, $V_z$ in GSM coordinates and the absolute value of the velocity are shown. As the trajectory is close to the equatorial GSM plane, the flow has strong $V_x$ and $V_y$ components, the $V_z$ component is small and varies in range -50 ÷ 50 km/s. The computed values of the directional components $V_x$ and $V_y$ coincide well with the registered ones – Fig.5 a,b. The model $V_z$ components differs more significantly from the observed values, but this component in itself is less than other components. Before the BS crossing at 16:03UT TH B is in the solar wind and measures the velocity of the solar wind. At the satellite's position, close to the terminator plane, the velocity in the magnetosheath is about 70% from the solar wind velocity – Fig. 4b, 5d.

Fig. 6 presents the observed and numerically calculated ion density at the points of the satellite's trajectory in the magnetosheath on 10-11 June 2009. We observe a good coincidence of the model-calculated and measured values of the density. We see in the magnetosheath an increase of the density by a factor of 2.6 compared to the unshocked solar wind - Fig. 4a. The density reaches its maximum at the bow shock, which is about 1.7 times higher than that at the magnetopause – Fig. 4a, Fig 6.

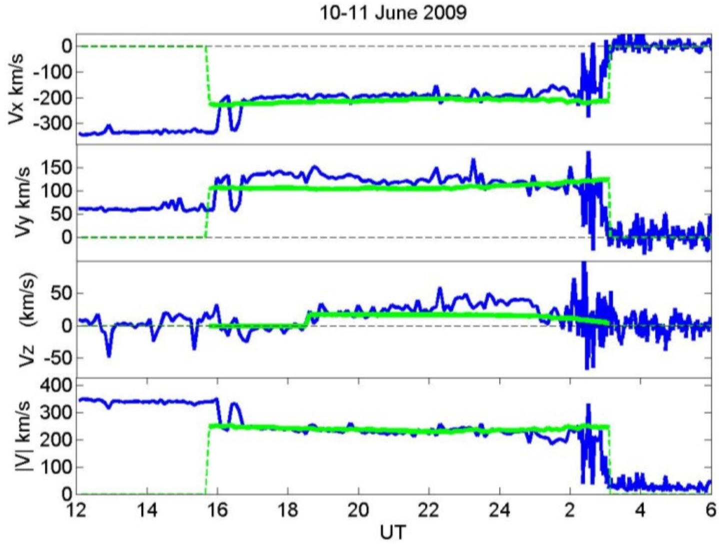


**Fig. 5.** Comparison between the measured plasma parameters (blue) and those, calculated by the model (green). From top to bottom: $V_x$, $V_y$ $V_z$, (GSM) components and |V| of the ion velocity.

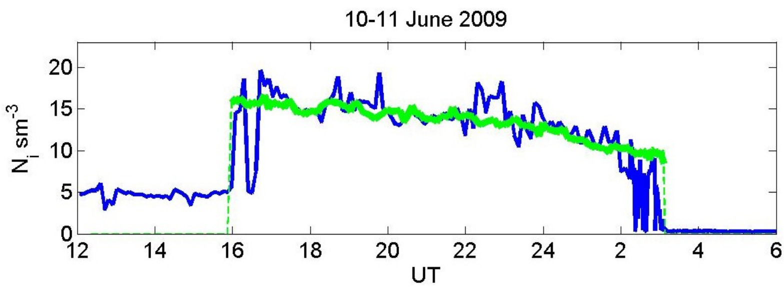


**Fig. 6.** Comparison between the measured (blue) and the numerically calculated (green) ion density.

## 4 Summary

This is a test of the model capabilities in the description of the behaviour of the plasma parameters in the magnetosheath. Here, data from the most recent space mission of THEMIS spacecraft were used. The model presented here is capable of describing the measured plasma parameters in the magnetosheath with great accuracy and may be used to interpret the phenomena, observed in the terrestrial magnetosheath.

The paper is supported by the Bulgarian National Council “Scientific Research” under Project DMU 03/88.

## References

1. J.R. Spreiter, A.L. Summers, A.Y. Alksne, Planet. Space. Sci. **14**, 223-253, (1966)
2. J.R. Spreiter, S.S. Stahara, J. Geophys. Res. **85**, 6769-6777, (1980)
3. J.R. Spreiter, S.S. Stahara, Adv. Sp. Res. **7**, 5-19, (1994)
4. T. Ogino, R.J. Walker, M. Ashour-Abdalla, J. Geophys. Res. **99**, 11027-11042, (1994)
5. M. Janhunen, T. Palmroth, I. Laitinen et al., J. Atm. Sol. Terr. Phys. **80**, 48-59, (2012)
6. J. Raeder, D. Larson, W. Li, E.L. Kepko, T. Fuller-Rowell, Space Sci. Rev. **141**, 535-555, (2008)
7. J.G. Lyon, J.A. Fedder, C.M. Mobarry, J. Atm. Sol. Terr. Phys. **66**, 1333-1350, (2004)
8. G. Toth, I.V. Sokolov, T.I. Gombosi et al., J. Geophys. Res. **110**, A12226, (2005)
9. K.G. Powell, P.L. Roe, T.J. Linde, T.I. Gombosi, D.L. De Zeeuw, J. Comput. Phys. **154**, 284-309, (1999)
10. P.S. Dobreva, M.D. Kartalev, M.D. Shevyrev, G.N. Zastenker, Planet. Sp. Sci. **53**, 117-125, (2005)
11. P.S. Dobreva, M.D. Kartalev, N.L. Borodkova, G.N. Zastenker, Adv. Sp. Res. **58**, 188-195, (2016)
12. A.S. Magomedov, K.M. Holodov, Grid Characteristic Numerical Method, Nauka, Moscow, (1988)
13. N.A. Tsyganenko, J. Geophys. Res. **100**, 5599-5612 , (1995)
14. N.A. Tsyganenko, J. Geophys. Res., **107**(A8), 10.1029/2001JA000219, (2002)
15. P.S. Dobreva, M.D. Kartalev, D. Koitchev, V.I. Keremidarska, M. Kaschiev, Adv. Sp. Res. **41**, 1279-1285, (2008)
16. M. Kartalev, P. Dobreva, E. Amata, M. Dryer, S. Savin, J. Atm. Sol. Terr. Phys. **70**(2-4), 627-636, (2008)
17. E.C. Stone, A.M Frandsen, R.A. Mewaldt et al., Space Sci. Rev. **86**(1-4), 1-22, (1998)
18. M.H. Acuna, K.W. Ogilvie, D.N. Baker, S.A. Curtis, D.H. Fairfield, W.H. Mish, Space Sci. Rev. **71**, 521, (1995)
19. K.W. Ogilvie, D.J. Chornay, R.J. Fritzenreiter et al., Space Sci. Rev. **71**, 41-54, (1995)
20. R.P. Lin, K.A. Anderson, , S. Ashford et al., Space Sci. Rev. **71**(1-4), 125-153, (1995)
21. R.P. Lepping, M.H. Acuna, L.F. Burlaga et al., Space Sci. Rev. **71**, 207-218, (1995)
22. V. Angelopoulos, Space Sci. Rev. **141**, 5-34, (2008)
23. D.G. Sibeck, V. Angelopoulos, Space Sci. Rev. **141**, 35-59, (2008)
24. J.-H. Shue, J.K. Chao, H.C. Fu et al., J. Geophys. Res. **102**(A5), 9497-9511, (1997)
25. J.P. McFadden, C.W. Carlson, D. Larson, M. Ludlam, R. Abiad et al., Space Sci. Rev. **141**(1-4), 277-302, (2008)